

# Dependence of the prompt fission $\gamma$ -ray spectrum on the entrance channel of compound nucleus: spontaneous vs neutron-induced fission

C.Y. Wu<sup>1</sup>, A. Chyzh<sup>2</sup>, P. Jaffke<sup>3</sup>, R.A. Henderson<sup>1</sup>, P. Talou<sup>3</sup>, I. Stetcu<sup>3</sup>, J. Henderson<sup>1</sup>, M.Q. Buckner<sup>1</sup>, S.A. Sheets<sup>1</sup>, R. Hughes<sup>1</sup>, B. Wang<sup>1</sup>, J.L. Ullmann<sup>4</sup>, S. Mosby<sup>4</sup>, T.A. Bredeweg<sup>5</sup>, A.C. Hayes-Sterbenz<sup>3</sup>, and J.M. O'Donnell<sup>4</sup>

<sup>1</sup> Lawrence Livermore National Laboratory, Livermore, California 94550, USA

<sup>2</sup> North Carolina State University, Raleigh, North Carolina 27695, USA

<sup>3</sup> Theoretical Division, Los Alamos National Laboratory, Los Alamos, New Mexico 87545, USA

<sup>4</sup> Physics Division, Los Alamos National Laboratory, Los Alamos, New Mexico 87545, USA

<sup>5</sup> Chemistry Division, Los Alamos National Laboratory, Los Alamos, New Mexico 87545, USA

## Abstract

Prompt  $\gamma$ -ray spectra were measured for neutron-induced fission of  $^{239,241}\text{Pu}$  with incident neutron energy from thermal to about 100 keV and spontaneous fission of  $^{240,242}\text{Pu}$  using the Detector for Advanced Neutron Capture Experiments (DANCE) array in coincidence with the detection of fission fragments by a parallel-plate avalanche counter. The unfolded prompt fission  $\gamma$ -ray spectra can be reproduced reasonably well by Monte Carlo Hauser-Feschbach statistical model for neutron-induced fission channel but not for the spontaneous fission channel. However, this entrance-channel dependence of the prompt fission  $\gamma$ -ray emission can be described qualitatively by the model due to the very different fission-fragment mass distributions and a lower average fragment spin for spontaneous fission. A supportive evidence is provided by the unfolded 2-D spectrum of total  $\gamma$ -ray energy vs multiplicity where the  $\gamma$ -ray multiplicity distribution has a tail extended to higher multiplicity for neutron-induced fission channel.

## 1 Introduction

The prompt energy released in the nuclear fission is dominated by the kinetic energy of the fission fragments and then followed by the prompt neutron and  $\gamma$ -ray emission from the fission fragments. In the past, most model and experimental efforts were devoted to the kinematic energy of fission fragments and the neutron emission. Little attention was paid to the  $\gamma$ -ray emission until recently. A single  $\gamma$ -ray detector was used for most measurements made in 1970's and their results were summarized in Refs. [1]. Recent years have seen an increased interest in the prompt  $\gamma$ -ray emission in fission [2-14] because the data are important for fission modeling and applications in nuclear industries. For example, new prompt fission  $\gamma$ -ray data at thermal neutron energy and above for  $^{235}\text{U}$  and  $^{239}\text{Pu}$ , required for the precise modeling of  $\gamma$ -ray heating in reactor cores, were categorized as high-priority by the Nuclear Energy Agency under the Organization for Economic Cooperation and Development [15].

Most measurements for the prompt  $\gamma$ -ray emission in fission were made using one or a few  $\gamma$ -ray detectors for the neutron-induced fission of U and Pu isotopes as well as  $^{252}\text{Cf}(\text{sf})$  and  $^{240,242}\text{Pu}(\text{sf})$ . More recently, a new class of fast scintillators, such as cerium-doped-LaBr<sub>3</sub>, CeBr<sub>3</sub>, and LaBr<sub>3</sub> detectors, was used by Billnert *et al.* [4], Oberstedt *et al.* [7,10,12,13], and Gatera *et al.* [14]. Lately, a new generation of measurements has emerged for the prompt  $\gamma$ -ray emission in fission that uses highly segmented  $4\pi$   $\gamma$ -ray calorimeters, such as the Heidelberg-Darmstadt Crystal Ball [16] and the Detector for Advanced Neutron Capture Experiments (DANCE) array [17,18].

Measurements of the prompt fission  $\gamma$ -ray emission for the cases mentioned above were made for either the neutron-induced fission at a given incident neutron energy or the spontaneous fission. No report was made for the impact of compound nucleus entrance channel on prompt fission  $\gamma$ -ray emission except for

a recent study of  $^{240,242}\text{Pu}$ , where the spontaneous fission was measured for  $\gamma$ -ray energy up to 4 MeV [13]. The comparison with thermal neutron-induced fission  $^{241}\text{Pu}(\text{n}_{\text{th}},\text{f})$  indicates no or little dependence on the entrance channel of the  $^{242}\text{Pu}^*$  compound nucleus. Furthermore, there are known cases where the prompt fission  $\gamma$ -ray spectra were measured using fast neutrons with energy up to 20 MeV for  $^{235}\text{U}(\text{n},\text{f})$  and  $^{238}\text{U}(\text{n},\text{f})$  [19,20] and no obvious dependence on the incident neutron energy was found. However, the measurement given in Refs. [21,22] showed that the prompt  $\gamma$ -ray spectrum for neutron-induced fission of  $^{238}\text{U}$  after the third-chance fission is different from those with lower incident neutron energy that can be described adequately by model calculations [23].

In this work, we present a new study of the dependence of prompt fission  $\gamma$ -ray emission on the entrance channels of  $^{240,242}\text{Pu}^*$  compound nuclei. There are two distinct entrance channels for their fission. One is spontaneous fission and has an entrance channel of zero intrinsic excitation energy and spin  $0^+$ . The second channel is neutron-induced fission of  $^{239,241}\text{Pu}$  with the incident neutron energy from thermal to 100 keV. They have the entrance channel of  $\approx 6.3$  MeV intrinsic excitation energy with spin of 0 or 1 for  $^{239}\text{Pu}(\text{n},\text{f})$  and  $\approx 6.5$  MeV intrinsic excitation energy with spin of 2 or 3 for  $^{241}\text{Pu}(\text{n},\text{f})$ . The prompt fission  $\gamma$ -ray emission for both fission channels of both compound nuclei was measured using the DANCE array in coincidence with the detection of fission fragments by a compact parallel-plate avalanche counter (PPAC) [24], designed specifically for DANCE. The description of experiments and data analysis as well as the discussion of results will be presented in the sections below. Some of the results have been published [25].

## 2 Experiments and data analysis

Measurements of the prompt  $\gamma$ -ray spectrum of  $^{239,241}\text{Pu}(\text{n},\text{f})$  and of  $^{240,242}\text{Pu}(\text{sf})$  were performed at the Lujan Neutron Scattering Center at LANL/LANSCE. For neutron-induced fission experiments, PPACs with either  $^{239}\text{Pu}$  or  $^{241}\text{Pu}$  targets were assembled at LLNL and bombarded by neutrons with energies from thermal up to several hundred keV. Neutrons were produced first by bombarding a tungsten target with an 800 MeV proton beam at a repetition rate of 20 Hz and then moderated by water. The prompt  $\gamma$  rays emitted in fission were detected by the DANCE array in coincidence with the detection of fission fragments by PPACs. A total of over  $10^6$  fission events with at least one  $\gamma$  ray detected by DANCE were collected for both isotopes. These results were published earlier [5,9]. For the spontaneous fission, PPACs with a total mass of about 642  $\mu\text{g}$  of  $^{242}\text{Pu}$  enriched to 99.93 % or about 769  $\mu\text{g}$  of  $^{240}\text{Pu}$  enriched to 98.86 % were assembled at LLNL and used for the fission-fragment detection in coincidence with the detection of the prompt  $\gamma$  rays by DANCE. A total of about  $10^5$  fission events with at least one  $\gamma$  ray detected by DANCE were collected for both targets.

In the offline analysis using the code FARE [26], a valid fission event required a coincidence between the detection of a fission fragment by the PPAC and the detection of  $\gamma$  rays by DANCE with an 8-10 ns time window on their time difference spectrum. A time resolution better than 2 ns was achieved for all fission reactions studied. Three physical quantities were inferred from the coincident  $\gamma$  rays detected by DANCE: (1) the total prompt fission  $\gamma$ -ray energy  $E_{\gamma,\text{tot}}$  spectrum defined as the sum of energy of all detected  $\gamma$  rays; (2) the total prompt fission  $\gamma$ -ray multiplicity  $M_{\gamma}$  spectrum determined according to the number of clusters, grouped adjacent detectors triggered; (Note that this counting method for  $M_{\gamma}$  avoids double counting due to the Compton scattering, is largely independent of the  $\gamma$ -ray energies  $E_{\gamma}$ , and is closer to the simulated results using  $\gamma$ -ray calibration sources [3,27,28]) (3) the prompt fission  $\gamma$ -ray energy  $E_{\gamma}$  spectrum determined by excluding any  $\gamma$  ray with adjacent crystals triggered to avoid the summing effect. Details of this analysis have been described in our earlier publications [3,5,9].

Corrections must be made to the measured spectra to obtain the actual physical ones that can be compared to model calculations. This can be accomplished by unfolding the measured spectra using the detector response matrices. For unfolding one-dimensional spectra such as  $E_{\gamma}$ , the iterative Bayesian [29,30,31] and the singular-value decomposition (SVD) [32] methods are available. The detector

response matrices are simulated using the GEANT4 [33] geometrical model including both DANCE and PPAC [3,5,9]. To make sure the simulated detector response matrices have sufficient coverage of the phase space beyond the measured one, we use the  $E_\gamma$  spectrum in the range 0.1-12 MeV for the response matrix in the unfolding.

For unfolding 2-D spectra such as  $E_{\gamma,\text{tot}}$  vs  $M_\gamma$ , the iterative Bayesian method is adopted. The value of  $M_\gamma$  up to 25 and  $E_{\gamma,\text{tot}}$  up to 40 MeV are included to have sufficient coverage of the phase space beyond the measured one, The  $E_{\gamma,\text{tot}}$  has a bin size of 200 keV and an energy threshold of 150 keV. So, the response matrix has a size of  $200 \times 25$ . For any given grid point ( $E_{\gamma,\text{tot}}$ ,  $M_\gamma$ ) in the response matrix, a two-dimensional DANCE response matrix of a size of  $200 \times 25$  is generated with a given assembly of no more than 20,000 samples. Note that the DANCE response to the total prompt  $\gamma$ -ray is relatively insensitive to the content of  $\gamma$  rays for a given sample since the  $\gamma$ -ray detection efficiency (84 to 88%) and the peak-to-total ratio ( $\sim 55\%$ ) remain nearly constant for the  $\gamma$ -ray energy ranging from 150 keV to 10 MeV [3,27,28]. Each sample has a matching number of  $\gamma$  rays to  $M_\gamma$ , selected randomly according to the unfolded  $E_\gamma$  distributions in Refs. [3,5] and this work with the condition on the total  $\gamma$ -ray energy that is equal to  $E_{\gamma,\text{tot}} \pm 100$  keV. This simulation is repeated for all the grid points within the lower and upper bound of  $E_{\gamma,\text{tot}}$  for a given  $M_\gamma$ , established by this random sampling technique.

### 3 Results and discussions

The unfolded  $E_\gamma$  spectra obtained by using the iterative Bayesian method, for  $^{240}\text{Pu}(\text{sf})$  as well as  $^{239}\text{Pu}(\text{n,f})$  are shown in Fig. 1(a), and the spectra for  $^{242}\text{Pu}(\text{sf})$  and  $^{241}\text{Pu}(\text{n,f})$  are shown in Fig. 1(b). A very similar trend is observed for fission of both compound nuclei; that is the  $E_\gamma$  spectrum for the spontaneous fission is harder than that of the neutron-induced fission for  $\gamma$ -ray energies above 2 MeV. The difference in yield is nearly a factor of 2 for  $\gamma$ -ray energy near 6 MeV. In general, the systematic uncertainty is about 10 % for the unfolding with simulated detector responses, which is an order of magnitude smaller than the observed difference in yield and has no impact on the conclusion.

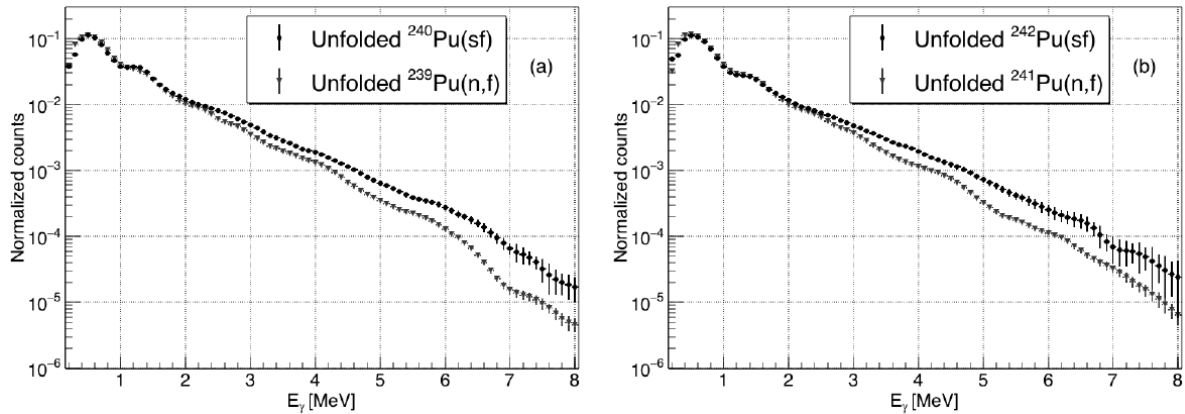


**Fig. 1** Comparison of unfolded  $E_\gamma$  spectrum between  $^{240}\text{Pu}(\text{sf})$  (black) and  $^{239}\text{Pu}(\text{n,f})$  (red) is shown in (a) and between  $^{242}\text{Pu}(\text{sf})$  (black) and  $^{241}\text{Pu}(\text{n,f})$  (red) shown in (b). All spectra are self-normalized to one.

We have used the CGMF code [8] to model the de-excitation of fission fragments through a Monte Carlo implementation of the statistical Hauser-Feshbach theory [34]. Both the prompt  $\gamma$ -ray observables as well as prompt neutron observables are calculated. These include the average prompt neutron multiplicity  $\langle \nu \rangle$ , its dependence on fragment mass  $\langle \nu \rangle(A)$ , and the distribution  $P(\nu)$ , as well as the average prompt  $\gamma$ -ray multiplicity  $\langle M_\gamma \rangle$  and prompt fission  $\gamma$ -ray energy  $E_\gamma$  spectrum (PFGS). The prompt neutron observables for  $^{239,241}\text{Pu}(\text{n,f})$  and  $^{240,242}\text{Pu}(\text{sf})$  are used to constrain the CGMF calculations. Details of the parameters used in the calculation and their sensitivities to the observables,

such as the total kinetic energy, fission-fragment mass and angular momentum distribution are described in Ref. [25] and elsewhere in this proceeding by P. Jaffke *et al.*.

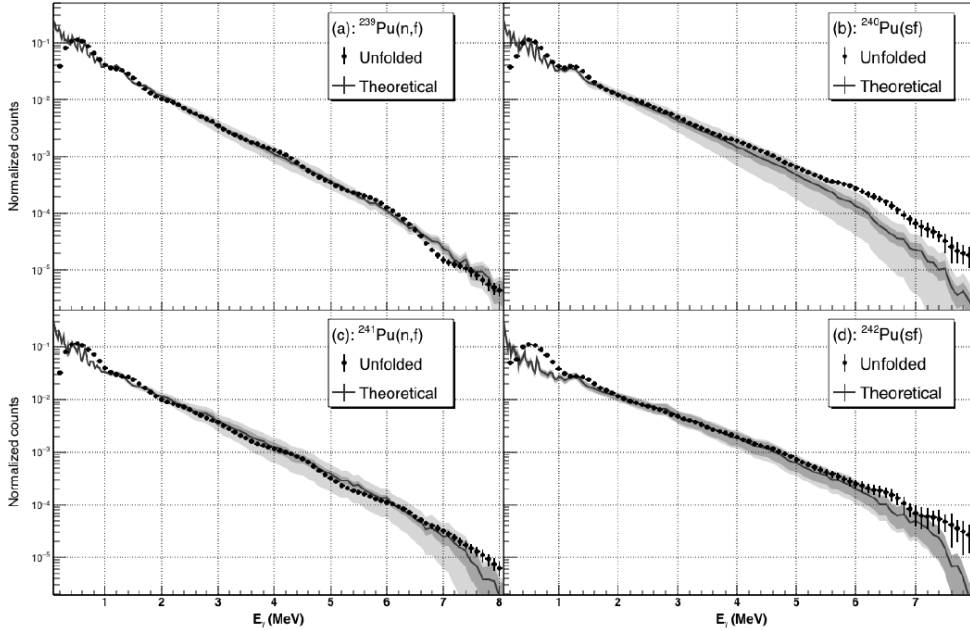


**Fig. 2** Comparison of the unfolded (points) and calculated (lines and bands) prompt fission  $\gamma$ -ray spectrum (PFGS) for  $^{239}\text{Pu}(n,f)$  (a),  $^{240}\text{Pu}(sf)$  (b),  $^{241}\text{Pu}(n,f)$  (c), and  $^{242}\text{Pu}(sf)$  (d). The calculated central values (lines) use the nominal total kinetic energy of the fragments  $\langle\text{TKE}\rangle_{\text{exp}}$  and the light (dark) bands are the  $\pm 0.5$  MeV ( $\pm 1.0$  MeV) uncertainties. Unfolded spectra are self-normalized to one. To account for a lack of experimental sensitivity below 1 MeV, calculated data were normalized to experimental data in the  $1 \leq E_{\gamma} \leq 5$  MeV range.

Plotted in Fig. 2 are the comparisons between the unfolded results from DANCE and the CGMF calculations. The lighter and darker bands indicate the calculated spectra when we vary  $\langle\text{TKE}\rangle_{\text{exp}}$  by  $\pm 0.5$  MeV and  $\pm 1.0$  MeV. We can see that the measured  $^{239}\text{Pu}(n,f)$  PFGS is reproduced nicely by the calculations, even up to  $E_{\gamma} \sim 7$  MeV. The  $^{240}\text{Pu}(sf)$  PFGS is reasonably well reproduced, but the slope is too steep. The  $^{241}\text{Pu}(n,f)$  calculation is slightly harder than the measured result, indicating that a lower  $\langle\text{TKE}\rangle$  than the used  $\langle\text{TKE}\rangle_{\text{exp}}$  could produce a better fit and a higher  $\langle M_{\gamma} \rangle$  as well, in agreement with Refs. [9,10]. The  $^{242}\text{Pu}(sf)$  PFGS can reproduce the unfolded data reasonably well, but the large  $\langle\text{TKE}\rangle_{\text{exp}}$  we have used generates a very small  $\langle M_{\gamma} \rangle \sim 4.2$   $\gamma$ /fission, far below the values in Refs. [1,13]. For both  $^{240}\text{Pu}^*$  and  $^{242}\text{Pu}^*$ , neutron-induced fission required a larger average angular momentum carried by the fission fragments to achieve good agreement with  $\langle\nu\rangle$ . Overall, the neutron-induced fission reactions are in better agreement than spontaneous fission. This is further supported by the observation of unfolded 2-D spectrum of  $E_{\gamma,\text{tot}}$  vs  $M_{\gamma}$  for  $^{242}\text{Pu}^*$  compound nucleus, shown in Fig 3, where the  $M_{\gamma}$  distribution has a tail stretched to higher multiplicity for neutron-induced fission channel.

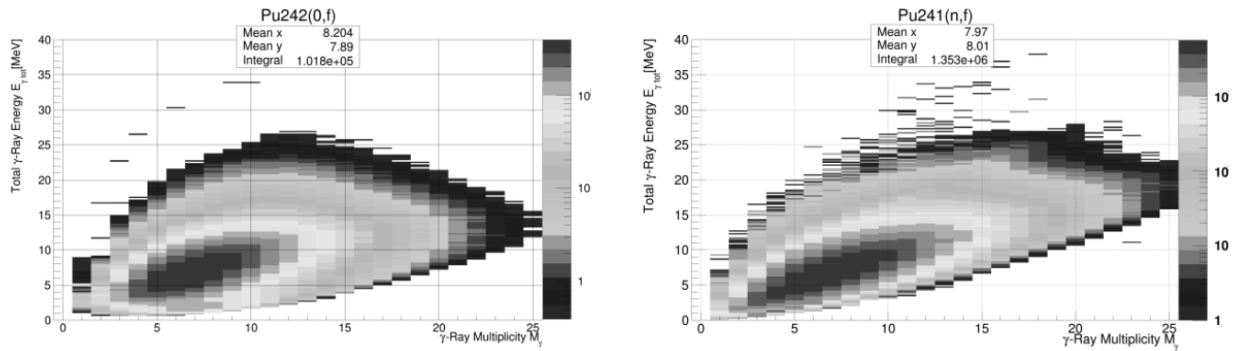


**Fig. 3** Comparison of the unfolded 2-D spectrum of the total  $\gamma$ -ray energy ( $E_{\gamma,\text{tot}}$ ) vs multiplicity ( $M_\gamma$ ) between spontaneous (L) and neutron-induced (R) fission of  $^{242}\text{Pu}^*$ . The  $M_\gamma$  multiplicity has a long tail toward higher multiplicity for neutron-induced fission channel.

## 4 Summary

In summary, the prompt  $\gamma$ -ray spectra of  $^{240,242}\text{Pu}(\text{sf})$  and  $^{239,241}\text{Pu}(\text{n,f})$  with the incident neutron energy range from thermal to  $\sim 100$  keV were measured using the DANCE array in coincidence with the detection of fission fragments using a PPAC. This offers an opportunity to study the dependence of prompt fission  $\gamma$ -ray emission on the entrance channel for the formation of the compound nucleus. It was carried out by comparing the unfolded experimental spectra and the ones calculated using the CGMF code, a Monte Carlo Hauser-Feshbach statistical model. The experimental results with DANCE observed a relative hardening in both the  $^{240}\text{Pu}^*$  and  $^{242}\text{Pu}^*$  compound systems. The observed differences in the  $E_\gamma$  spectrum between the spontaneous and neutron-induced fission were qualitatively confirmed by the model calculations and interpreted as due to the difference in the fission-fragment mass distributions and fragment spin distributions. The mass distributions for spontaneous fission peak near  $A \sim 133$  and has a narrower variance, where the average  $\gamma$ -ray energies are known to increase. A portion of the observed hardening of the  $E_\gamma$  spectrum relative to the neutron-induced reaction for the  $^{242}\text{Pu}^*$  and  $^{240}\text{Pu}^*$  compound system can be attributed to this change in mass distributions. A decrease in the average angular momentum carried by fission fragments for the spontaneous fission reactions could account for most of the observed differences in the prompt  $\gamma$ -ray spectra. Additional evidence to support this explanation is provided by the unfolded 2-D spectrum of  $E_{\gamma,\text{tot}}$  vs  $M_\gamma$  where the  $\gamma$ -ray multiplicity shows a tail extended to higher multiplicity for neutron-induced fission channel.

## Acknowledgement

This work benefited from the use of the LANSCE accelerator facility as was performed under the auspices of the US Department of Energy by Lawrence Livermore National Security, LLC under contract DE-AC52-07NA27344 and by Los Alamos National Security, LLC under contract DE-AC52-06NA25396. Funding also is acknowledged from the U.S. DOE/NNSA Office of Defense Nuclear Nonproliferation Research and Development and DOE/SC Office of Nuclear Physics. All isotopes used in the measurements were obtained from Oak Ridge National Laboratory.

## References

- [1] T.E. Valentine, *Annals of Nuclear Energy* 28, 191 (2001).
- [2] A. Hotzel *et al.*, *Z Phys.* A356 (1996) 299.
- [3] A. Chyzh, C.Y. Wu, E. Kwan, R.A. Henderson, J.M. Gostic, T.A. Bredeweg, R.C. Haight, A.C. Hayes-Sterbenz, M. Jandel, J.M. O'Donnell *et al.*, *Phys. Rev. C* 85 (2012) 021601(R).
- [4] R. Billnert, F.-J. Hamsch, A. Oberstedt, and S. Oberstedt, *Phys. Rev. C* 87 (2013) 024601.
- [5] A. Chyzh, C.Y. Wu, E. Kwan, R.A. Henderson, J.M. Gostic, T.A. Bredeweg, A. Couture, R.C. Haight, A.C. Hayes-Sterbenz, M. Jandel *et al.*, *Phys. Rev. C* 87 (2013) 034620.

- [6] J.L. Ullmann, E.M. Bond, T.A. Bredeweg, A. Couture, R.V. Haight, M. Jandel, T. Kawano, H.Y. Lee, J.M. O'Donnell, A.C. Hayes *et al.*, Phys. Rev. C 87 (2013) 044607.
- [7] A. Oberstedt *et al.*, Phys. Rev. C 87 (2013) 051602(R).
- [8] B. Becker, P. Talou, T. Kawano, Y. Danon, and I. Stetcu, Phys. Rev. C 87 (2013) 014617.
- [9] A. Chyzh, C.Y. Wu, E. Kwan, R.A. Henderson, T.A. Bredeweg, R.C. Haight, A.C. Hayes-Sterbenz, H.Y. Lee, J.M. O'Donnell, and J.L. Ullmann, Phys. Rev. C 90 (2014) 014602.
- [10] A. Oberstedt *et al.*, Phys. Rev. C 90 (2014) 024618.
- [11] I. Stetcu, P. Talou, T. Kawano, and M. Jandel, Phys. Rev. C 90 (2014) 024617.
- [12] A. Oberstedt, R. Billnert, F.-J. Hamsch, and S. Oberstedt, Phys. Rev. C 92 (2015) 014618.
- [13] S. Oberstedt, A. Oberstedt, A. Gatera, A. Gook, F.-J. Hamsch, and A. Moens, G. Sibbens, D. Vanleeuw, and M. Vidali, Phys. Rev. C 93 (2016) 054603.
- [14] A. Gatera *et al.*, Phys. Rev. C 95 (2017) 064609.
- [15] Nuclear Data High Priority Request List of the NEA (Req. ID: H.3, H4).
- [16] V. Metag *et al.*, in *Proceedings of the Symposium on Detectors in heavy-ion Reactions, Berlin 1982*, edited by V. Oertzen, Lect. Notes Phys. 178 (Springer, Berlin, 1983) p. 163.
- [17] M. Heil, R. Reifarh, M. M. Fowler, R. C. Haight, F. Kappeler, R. S. Rundberg, E. H. Seabury, J. L. Ullmann, and K. Wisshak, Nucl. Instrum. Methods in Phys. Res. A 459 (2001) 229.
- [18] R. Reifarh *et al.*, IEEE Transactions on Nuclear Science 53 (2006) 880.
- [19] E. Kwan *et al.*, Nucl. Instrum. Methods Phys. Res. A 688 (2012) 55.
- [20] M. Lebois *et al.*, Phys. Rev. C 92 (2015) 034618.
- [21] J.M. Laborie, G. Belier, and J. Taieb, Phys. Proc. 31 (2012) 13.
- [22] J.M. Laborie, G. Belier, J. Taieb, A. Oberstedt, S. Oberstedt, Eur. Phys. Jour. Web of Conferences 146 (2017), 04032.
- [23] A. Oberstedt, R. Billnert, and S. Oberstedt, Phys. Rev. C 96 (2017) 034612.
- [24] C.Y. Wu, A. Chyzh, E. Kwan, R. Henderson, J. Gostic, D. Carter, T. Bredeweg, A. Couture, M. Jandel, J. Ullmann, Nucl. Instrum. Methods Phys. Res. A 694 (2012) 78.
- [25] A. Chyzh, P. Jaffke, C.Y. Wu, R.A. Henderson, P. Talou, I. Stetcu, J. Henderson, M.Q. Buckner, S.A. Sheets, R. Hughes, B. Wang, J.L. Ullmann, S. Mosby, T.A. Bredeweg, A.C. Hayes-Sterbenz, and J.M. O'Donnell, Phys. Lett. B 782 (2018) 652.
- [26] M. Jandel, T.A. Bredeweg, A. Couture, J.M. O'Donnell, and J.L. Ullmann, Los Alamos National Laboratory, LA-UR-12-21171 (2012).
- [27] R. Reifarh *et al.*, Los Alamos National Laboratory, LA-UR-01-4185 (2001).
- [28] R. Reifarh *et al.*, Los Alamos National Laboratory, LA-UR-03-5560 (2003).
- [29] G. D'Agostini, Nucl. Instrum. Methods Phys. Res. A362, 487 (1995).
- [30] G. D'Agostini, arXiv: 1010.0612 (2010).
- [31] T.J. Adye, arXiv: 1105.1160 (2011).
- [32] A. Hocker and V. Kartvelishvili, Nucl. Instrum. Methods Phys. Res. A 372, 469 (1996).
- [33] S. Agostinelli *et al.*, Nucl. Instrum. Methods Phys. Res. A 506 (2003) 550.
- [34] W. Hauser and H. Feshbach, Physical Review 87, 2 (1952).